Tuning Optical Properties of Erbium-Doped Zinc-Sodium Tellurite Glass Via Incorporation of Gold Nanoparticles

Reuben Ho Chee Wui[1], Asmahani Awang[1]*, Alvie Lo Sin Voi[1], Chee Fuei Pien[1], Noraini Abdullah[2], Jedol Dayou[1]

1 Energy, Vibration and Sound Research Group (e-VIBS), Faculty of Science and Natural Resources, Universiti Malaysia Sabah, Jalan UMS, 88400 Kota Kinabalu, Sabah, MALAYSIA.
2 Mathematics With Economics Programme, Faculty of Science and Natural Resources, Universiti Malaysia Sabah, Jalan UMS, 88400 Kota Kinabalu, Sabah, MALAYSIA.
*Corresponding author. E-Mail: asmahani_awang@yahoo.com; Tel: +6088-320000. Ext.: 5584; Fax: +6-088-435324.

ABSTRACT

Glasses with composition of $70TeO_2$-$20ZnO$-$10Na_2O$-$0.5Er_2O_3$-(x) Au where x=0.0, 0.1, 0.3 and 0.4 mol% are synthesized via melt-quenching technique. Optical characterization is performed using UV-Vis spectroscopy. Ten absorption peaks are evidenced at 379 nm, 406 nm, 443 nm, 452 nm, 489 nm, 522 nm, 544 nm, 653 nm, 800 nm and 975 nm correspond to Er^{3+} transitions of $^4I_{15/2}\rightarrow{}^4G_{11/2}$, $^4I_{15/2}\rightarrow{}^2H_{9/2}$, $^4I_{15/2}\rightarrow{}^4F_{3/2}$, $^4I_{15/2}\rightarrow{}^4F_{5/2}$, $^4I_{15/2}\rightarrow{}^4F_{7/2}$, $^4I_{15/2}\rightarrow{}^2H_{11/2}$, $^4I_{15/2}\rightarrow{}^4S_{3/2}$, $^4I_{15/2}\rightarrow{}^4F_{9/2}$, $^4I_{15/2}\rightarrow{}^4I_{9/2}$ and $^4I_{15/2}\rightarrow{}^4H_{1/2}$, respectively. Direct band gap (E_{dir}), indirect band gap (E_{indir}) and Urbach energy (E_U) are estimated to be 3.403-3.420 eV, 3.131-3.198 eV and 0.152-0.180 eV respectively. The E_{dir}, E_{indir} and E_U parameters vary as gold nanoparticles (Au NPs) are incorporated into glass matrix and this leads to the generation of non-bridging oxygen, subsequently changing the structure of glass.

KEYWORDS: Nanoparticles; direct band gap; indirect band gap; Urbach energy; non-bridging oxygen

Received 28 February 2017 **Revised** 14 September 2017 **Accepted** 15 September 2017 **Online** 16 October 2017

INTRODUCTION

Tellurite glasses have some advantages over other types of glasses. They have relatively low phonon energy (≈750 cm^{-1}), high refractive index (≈2.0), high solubility of rare earth ions, etc. (Żmojda *et al*., 2014; Lin *et al*., 2008). Tellurite glass is a conditional glass former and incorporation of glass modifiers like rare earth metal oxide forms a stable glass (Parveen *et al*., 2016; El-Mallawany *et al*., 2008). The incorporation of glass modifiers changes the structural and optical properties of the glasses (Sidek *et al*., 2015; Wang *et al*., 2009; Elkhoshkhany *et al*., 2014; El-Mallawany, 2000).

Pure tellurite glass is made up of TeO_4 trigonal bipyramidal (tbp) units with bridging oxygen. In TeO_4 tbp unit, two oxygen atoms are in the axial site while the other two and a lone electron pair of tellurium are in three equatorial sites of the TeO_4 tbp unit. The incorporation of modifier into pure tellurite glass leads to the rupture of TeO_4 tbp, forming the TeO_{3+1} and/or TeO_3 trigonal pyramid (tp) unit (Dimitriev *et al*., 1983; Yusoff *et al*., 2015). TeO_3 unit has non-bridging oxygen. According to previous studies, modification in the glass structure leads to changes in direct optical band gaps, indirect optical band gaps and Urbach energy of glass (Dimitriev *et al*., 1983; El-Diasty *et al*., 2006; Jlassi *et al*., 2011; Sidek *et al*., 2009). In the present study, we investigate the effect of Au NPs on optical properties of the glass using small increment in the concentration of Au NPs.

BACKGROUND THEORY

Beer-Lambert law shows the amount of light absorbed by a material with thickness by comparing the intensity of transmitted light to intensity of incident light after the light passes

through the material. According to El-Mallawany (2000), the light is normally incident on the material surface in UV-Vis-NIR spectroscopy. Beer-Lambert law is given by:

$$\alpha = \frac{1}{d}\ln\frac{I_0}{I} \tag{1}$$

where α is absorption coefficient of the glass sample in the unit of cm^{-1}, d is thickness of the glass sample, I_0 is intensity of incident light, I is intensity of transmitted light, and $\ln\frac{I_0}{I}$ is absorbance (Ghoshal *et al*., 2015).

Davis-Mott relation shows the relationship between the absorption coefficient of an amorphous material and photon energy of the incident electromagnetic wave, and also enables calculation of optical band gaps. Accordingly, Tauc plot derived from Davis-Mott relation gives the absorption coefficient of the glass as a function of photon energy for direct and indirect optical transitions (El-Diasty *et al*., 2006; El-Mallawany *et al*., 2008; Jlassi *et al*., 2011):

$$\alpha(\omega) = \frac{A(\hbar\omega - E_{opt})^n}{\hbar\omega} \tag{2}$$

where A is an energy-independent constant, E_{opt} is optical band gap, $\hbar\omega$ is photon energy, and n is a constant which can be 1/2, 3/2, 2 or 3, depending on the type of optical transition. n equals to 1/2 for allowed direct transitions, 3/2 for forbidden direct transitions, 2 for allowed indirect transitions, and 3 for forbidden indirect transitions. By changing equation (2) into equation (3), a direct optical band gap of each glass sample can be determined. To determine indirect optical band gap of the glass, equation (4) is used.

$$(\alpha\hbar\omega)^2 = A(\hbar\omega - E_{opt}) \tag{3}$$

$$(\alpha\hbar\omega)^{1/2} = A(\hbar\omega - E_{opt}) \tag{4}$$

where E_{opt} is direct optical band gap for equation (3) when n equals to 1/2, and E_{opt} is indirect optical band gap for equation (4) when n equals to 2.

Urbach energy is a measure of the disorder of structure of the material. Urbach rule shows the exponential dependence of the absorption coefficient of a material on photon energy and enables calculation of Urbach energy. Urbach law gives exponential dependence of the absorption coefficient with photon energy given by equation (5) (Jlassi *et al*., 2011; Saritha *et al*., 2008; Soltani *et al*., 2016):

$$\alpha(\omega) = \alpha_0 \exp\left(\frac{\hbar\omega}{E_U}\right) \tag{5}$$

where α is absorption coefficient as a function of photon frequency, α_0 is a constant, E_U is Urbach energy, and $\omega = 2\pi f$ is angular frequency of photon with f (photon frequency) (Awang *et al*., 2013). By changing equation (5) into equation (6), this gives Urbach plot, and Urbach energy of each glass sample can be determined (Saritha *et al*., 2008).

$$\ln\alpha = \frac{\hbar\omega}{E_U} + \ln\alpha_0 \tag{6}$$

METHODOLOGY

Sample Preparation

Glass samples with composition $70TeO_2$-$20ZnO$-$10Na_2O$-$0.5Er_2O_3$-(x)Au where x=0.0, 0.1, 0.3 and 0.4 mol% were prepared by using melt-quenching technique. Table 1 shows the glass composition of respective glass. The glass ingredients were mixed thoroughly. They were put in a platinum crucible in a furnace at 900°C for 25 minutes, and then melted before pouring it into a brass mould. Next, the sample was put into an annealing furnace for 3 hours at 295°C to eliminate thermal and mechanical strains. The samples were gradually cooled down to room temperature before cutting and polishing prior to optical characterization. The bulk glass samples have a thickness of approximately 2 mm.

Table 1. Glass compositions and glass codes.

Glass codes	Glass composition (mol%)				
	TeO_2	ZnO	Na_2O	Er_2O_3	Au
TZNE0.5	70	20	10	0.5	0.0
TZNE0.5-Au 0.1	70	20	10	0.5	0.1
TZNE0.5-Au 0.3	70	20	10	0.5	0.3
TZNE0.5-Au 0.4	70	20	10	0.5	0.4

Sample Characterization

UV-Vis-NIR spectra are recorded by using Agilent Technologies Cary 60 UV-Vis spectrophotometer in the wavelength range of 300-1100 nm at room temperature.

RESULT AND DISCUSSION

UV-Vis-NIR Spectroscopy

Figure 1 represents UV-vis absorption spectra of the glass samples with varying concentration of Au NPs. Ten absorption peaks and their corresponding erbium transitions are summarized in Table 2. Addition of Au NPs does not change the positions of absorption peaks. This is likely because the concentration of Au NPs in the samples is very low (Dousti *et al*., 2015).

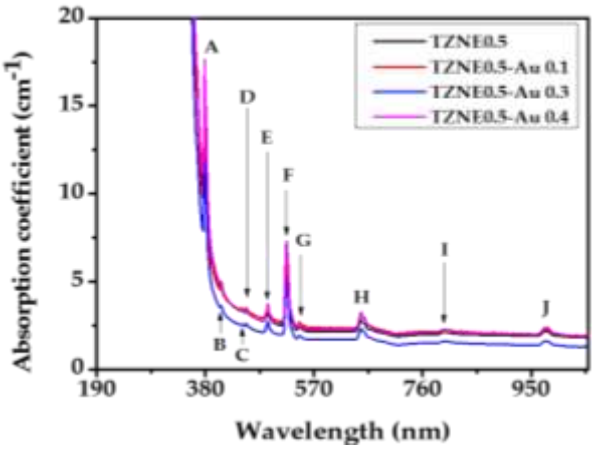

Figure 1. UV-Vis-NIR spectra of glass samples with different concentration of Au NPs.

Table 2. Absorption peaks and their corresponding peak labels, peak positions and transition of Er^{3+} ion from the ground state to excited state of energy levels.

Peak label	Peak position (nm)	Transition of Er^{3+} ion from ground state to an excited energy level	References
A	379	$^4I_{15/2}\rightarrow{}^4G_{11/2}$	Anigrahawati *et al*., 2015 Dousti *et al*., 2015 Serqueira *et al*., 2013
B	406	$^4I_{15/2}\rightarrow{}^2H_{9/2}$	Anigrahawati *et al*., 2015 Dousti *et al*., 2015 Serqueira *et al*., 2013
C	443	$^4I_{15/2}\rightarrow{}^4F_{3/2}$	Mahraz *et al*., 2014 Serqueira *et al*., 2013
D	452	$^4I_{15/2}\rightarrow{}^4F_{5/2}$	Baki *et al*., 2013 Serqueira *et al*., 2013
E	489	$^4I_{15/2}\rightarrow{}^4F_{7/2}$	Awang *et al*., 2015 Anigrahawati *et al*., 2015 Ghoshal *et al*., 2015 Serqueira *et al*., 2013
F	522	$^4I_{15/2}\rightarrow{}^2H_{11/2}$	Awang *et al*., 2015 Anigrahawati *et al*., 2015 Ghoshal *et al*., 2015 Serqueira *et al*., 2013
G	544	$^4I_{15/2}\rightarrow{}^4S_{3/2}$	Anigrahawati *et al*., 2015 Baki *et al*., 2013 Dousti *et al*., 2015 Dousti *et al*., 2015 Serqueira *et al*., 2013
H	653	$^4I_{15/2}\rightarrow{}^4F_{9/2}$	Awang *et al*., 2015 Anigrahawati *et al*., 2015 Ghoshal *et al*., 2015 Serqueira *et al*., 2013
I	800	$^4I_{15/2}\rightarrow{}^4I_{9/2}$	Awang *et al*., 2015 Anigrahawati *et al*., 2015 Ghoshal *et al*., 2015 Serqueira *et al*., 2013
J	975	$^4I_{15/2}\rightarrow{}^4I_{11/2}$	Awang *et al*., 2013 Anigrahawati *et al*., 2015 Ghoshal *et al*., 2015 Serqueira *et al*., 2013

Table 3 shows the variation in direct optical band gap, indirect optical band gaps and Urbach energy with increasing concentration of Au NPs. Figure 2(a) is a Tauc plot for determining the direct optical band gaps of the glass by using equation (3). Figure 2(b) shows that direct optical band gap of each glass sample is calculated by firstly extrapolating a straight line from the linear part of the Tauc plot until the straight line intersects with the photon energy axis where $(\alpha\hbar\omega)^2=0$ and subsequently calculating the gradient and y-intercept of the straight line (El-Diasty *et al*., 2006; Jlassi *et al*., 2011). The direct optical band gap equals to $-\frac{\text{y - intercept}}{gradient}$. Figure 2(c) shows the variation in direct optical

band gap with the addition of Au NPs in the glass samples. Upon addition of 0.1 mol% of Au NPs into the glass, direct optical band gap increases from 3.409 eV to 3.420 eV due to structural rearrangement of glass structure (Fatimah *et al*., 2014). This increase in direct optical band gap is also due to strengthening of covalency of oxygen ions, and change in oxygen bond strength in the glass structure as Au NPs are added. In other words, the excited electrons are tightly bound to bridging oxygen (BO) than NBO (Ahmadi *et al*., 2017). However, further addition of Au NPs from 0.1 to 0.4 mol% leads to the decreasing of direct optical band gap to 3.403 eV due to the creation of non-bridging oxygen (NBO) which changes the glass structure (Awang *et al*., 2013; Ghoshal *et al*., 2015; Soltani *et al*., 2016). Furthermore, low bonding energies of NBO also decrease the direct optical band gap (Yusof *et al*., 2015).

Table 3. Direct optical band gap (E_{dir}, eV), indirect optical band gap (E_{indir}, eV) and Urbach energy (E_U, eV) of each glass sample with different concentration of Au NPs.

Glass codes	E_{dir}	E_{indir}	E_U
TZNE0.5	3.409	3.151	0.173
TZNE0.5-Au 0.1	3.420	3.198	0.152
TZNE0.5-Au 0.3	3.418	3.190	0.154
TZNE0.5-Au 0.4	3.403	3.131	0.180

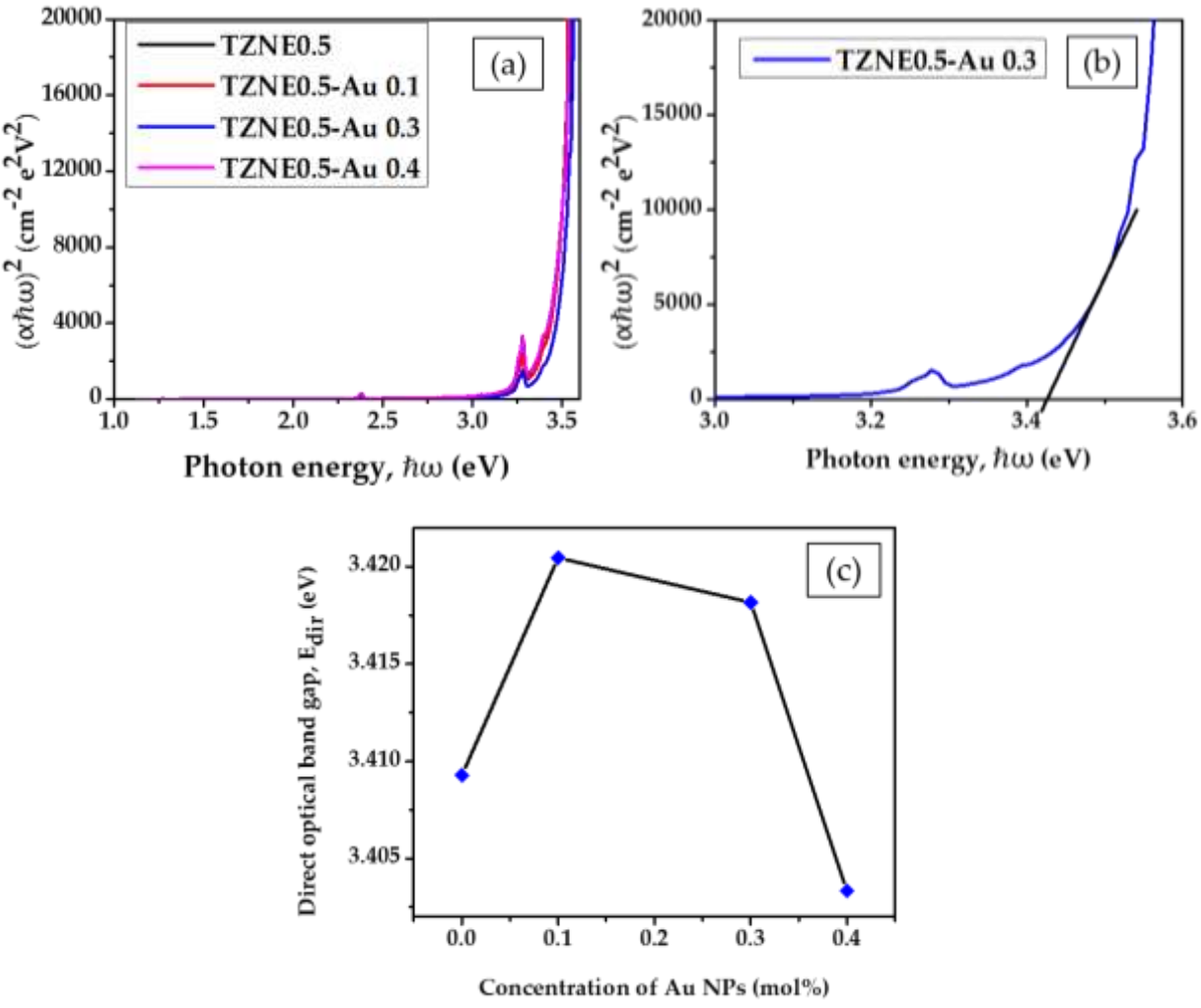

Figure 2. (a) Tauc plot for allowed direct transition; (b) TZNE0.5-Au 0.3 graph for calculating direct optical band gap; and (c) variations of direct optical band gap with varying concentration of Au NPs.

Figure 3(a) is a Tauc plot for determining indirect optical band gaps of the glass samples by using equation (4). Figure 3(b) is an example to show that indirect optical band gap of each sample is calculated by firstly extrapolating a straight line from the linear part of the Tauc plot until the straight line intersects with x-axis and then calculating the gradient and y-intercept of the straight line (El-Diasty *et al*., 2006; Jlassi *et al*., 2011). The indirect optical band equals to $-\frac{\text{y-intercept}}{gradient}$ when $(\alpha\hbar\omega)^{1/2}=0$. Figure 3(c) depicts the variation in indirect optical band gap with increasing the concentration of Au NPs. The addition of 0.1 mol% Au NPs leads to the increase in the optical band gap from 3.151 eV to 3.198 eV due to structural rearrangement (Fatimah *et al*., 2014). This increase in indirect optical band gap is also due to strengthening of covalency of oxygen ions, and change in oxygen bond strength in the glass structure upon addition of Au NPs (Ahmadi *et al*., 2017). In addition, the incorporation of Au NPs decreases the number of NBO and then makes glass structure more compact (Samanta *et al*., 2017). Nevertheless, increasing the concentration of Au NPs from 0.1 mol% to 0.4 mol% causes the indirect optical band gap to decrease from 3.190 eV to 3.131 eV due to the creation of NBO by the addition of Au NPs via conversion from TeO_4 tbp (trigonal bi-pyramidal) to TeO_3 tp (trigonal pyramidal) units, and low bonding energies of NBO (Ghoshal *et al*., 2015; Samanta *et al*., 2017; Soltani *et al*., 2016; Yusof *et al*., 2015; Yusoff *et al*., 2015).

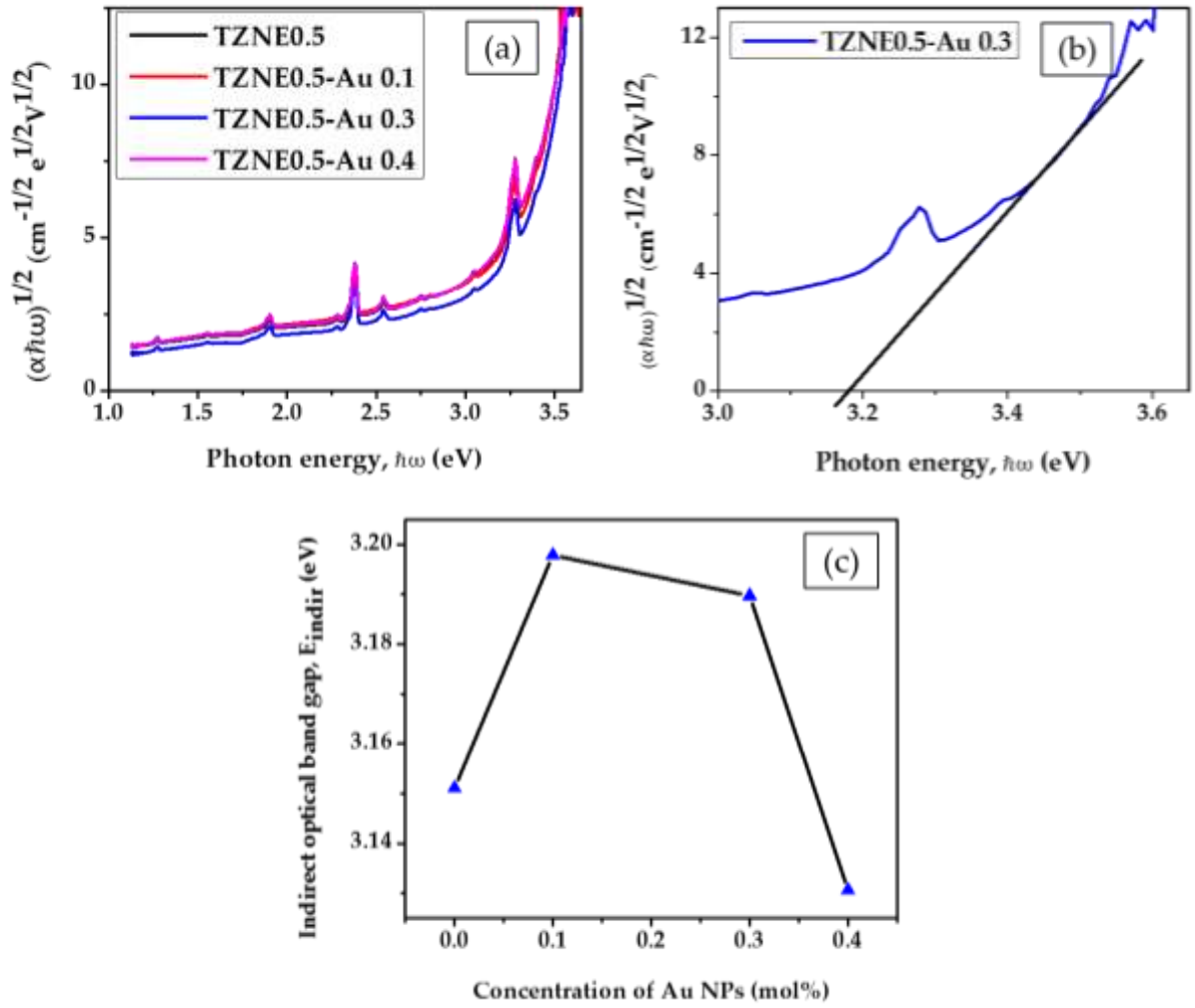

Figure 3. (a) Tauc plot for allowed indirect transition; (b) TZNE0.5-Au 0.3 graph for calculating indirect optical band gap; and (c) variations of indirect optical band gap with varying concentration of Au NPs.

Figure 4 (a) shows the Urbach plot for determining Urbach energy of each sample by using equation (6). Figure 4(b) is an example to show that Urbach energy is calculated by extrapolating a straight line from the linear part of the Urbach plot until the straight line intersects with photon energy axis where ln α=0 after calculating the gradient of the straight line (El-Diasty *et al*., 2006 ; Jlassi *et al*., 2011). Urbach energy is reciprocal of the gradient of the straight line, i.e. $\frac{1}{gradient}$. Figure 4 (c) shows the variations of Urbach with varying concentration of Au NPs. Adding 0.1 mol% of Au NPs into the glass decreases the Urbach energy from 0.173 eV to 0.152 eV due to structural rearrangement of glass structure and this leads to decrease in disorder of the glass structure (Fatimah *et al*., 2014). Further addition of Au NPs increases the Urbach energy from 0.154 eV to 0.180 eV because this causes the creation of non-bridging oxygen in the glass structure and hence the increase of the disorder of the glass structure (Ghoshal *et al*., 2015; Awang *et al*., 2013; Rivera *et al*., 2016; Yusoff *et al*., 2015).

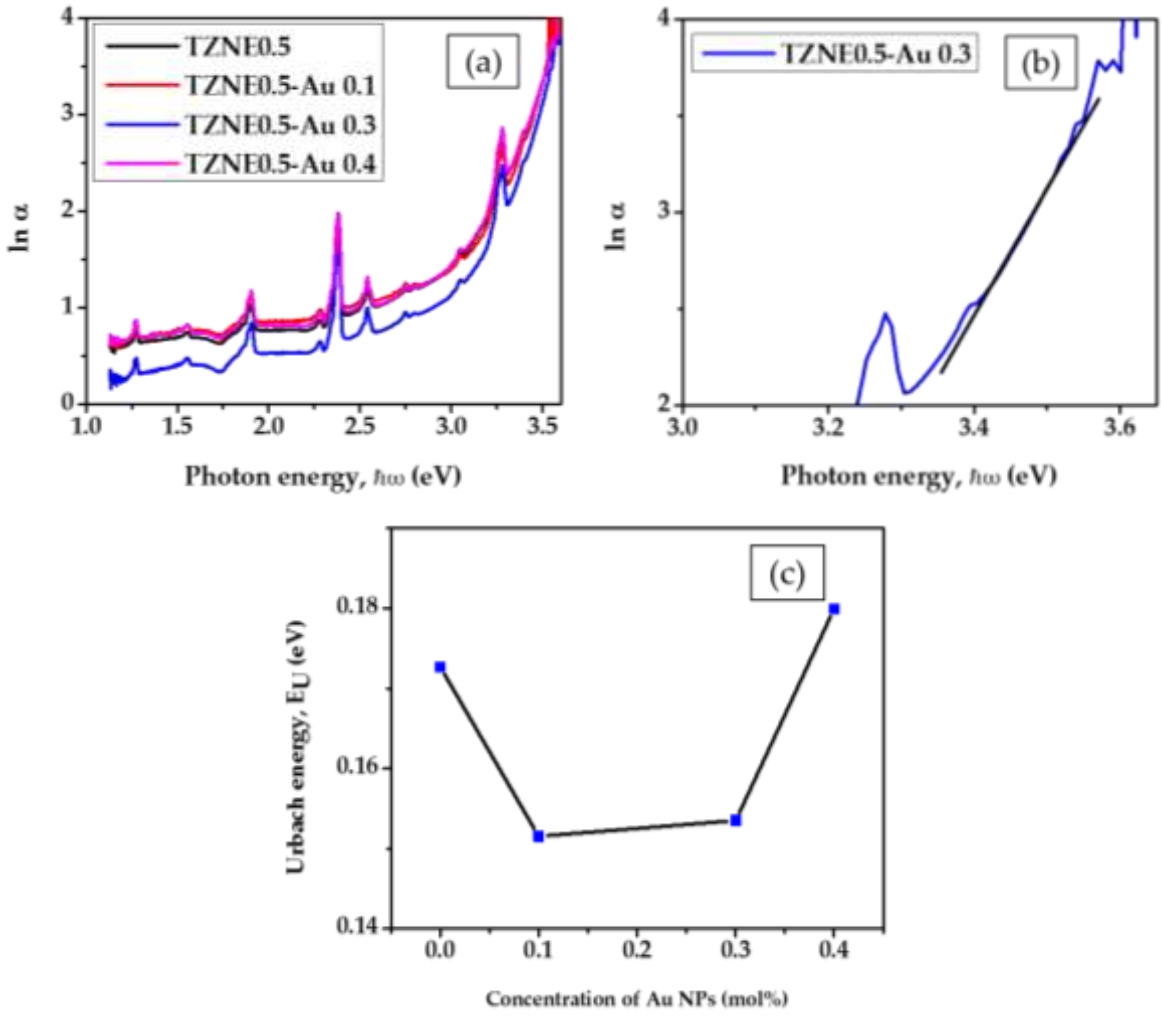

Figure 4. (a) Urbach plot of glass samples; (b) TZNE0.5-Au 0.3 graph for calculating Urbach energy; and (c) variations of Urbach energy with varying concentration of Au NPs.

CONCLUSION

The effect of changing the concentration of Au NPs on band gaps and Urbach energy of erbium-doped tellurite glass was studied. The addition of more Au NPs in the glass causes initially increase in band gaps and decrease in Urbach energy due to structural rearrangement of the structure

of the glass. Further increase in the concentration of Au NPs in the glass leads to the reduction in band gaps and increase in Urbach energy due to increasing disorder of glass structure via the creation of non-bridging oxygen by Au NPs to change the structure of the glass.

ACKNOWLEDGEMENTS

The authors wish to thank Universiti Malaysia Sabah and Ministry of Higher Education Malaysia for the financial support through SGPUMS (Vote SGK0008-SG-2015) and RAG0067-SG-2015.

REFERENCES

[1] Ahmadi, F., Hussin, R. & Ghoshal, S. K. (2017). Spectroscopic attributes of Sm^{3+} doped magnesium zinc sulfophosphate glass: Effect of silver nanoparticles inclusion. *Optical Materials*, **73**, 268-276.

[2] Anigrahawati, P., Sahar, M. R. & Ghoshal, S. K. (2015). Influence of Fe_3O_4 nanoparticles on structural, optical and magnetic properties of erbium doped zinc phosphate glass. *Materials Chemistry and Physics*, **155**, 155-161.

[3] Awang, A., Ghoshal, S. K., Sahar, M. R., Dousti, M. R., Amjad, R. J., & Nawaz, F. (2013). Enhanced spectroscopic properties and Judd-Ofelt parameters of Er-doped tellurite glass: Effect of gold nanoparticles. *Current Applied Physics*, **13**(8), 1813-1818.

[4] Awang, A., Ghoshal, S. K., Sahar, M. R., & Arifin, R. (2015). Gold nanoparticles assisted structural and spectroscopic modification in Er^{3+}-doped zinc sodium tellurite glass. *Optical Materials*, **42**, 495-505.

[5] Baki, S. O., Tan, L. S., Kan, C. S., Kamari, H. M., Noor, A. S. M. & Mahdi, M. A. (2013). Structural and optical properties of Er^{3+}-Yb^{3+} codoped multicomposition TeO_2-ZnO-PbO-TiO_2-Na_2O glass. *Journal of Non-Crystalline Solids*, **362**, 156-161.

[6] Dimitriev, Y., Dimitrov, V. & Arnaudov, M. (1983). IR spectra and structures of tellurite glasses. *Journal of Materials Science*, **18**(5), 1353-1358.

[7] Dousti, M. R., Amjad, R. J., Sahar, M. R., Zabidi, Z. M., Alias, A. N. & de Camargo, A. S. S. (2015). Er^{3+}-doped zinc tellurite glasses revisited: Concentration dependent chemical durability, thermal stability and spectroscopic properties. *Journal of Non-Crystalline Solids*, **429**, 70-78.

[8] Dousti, M. R., Amjad, R. J., & Mahraz, Z. A. S. (2015). Enhanced green and red upconversion emissions in Er^{3+}-doped boro-tellurite glass containing gold nanoparticles. *Journal of Molecular Structure*, **1079**, 347-352.

[9] Elkhoshkhany, N., Abbas, R., El-Mallawany, R., & Fraih, A. J. (2014). Optical properties of quaternary TeO_2-ZnO-Nb_2O_5-Gd_2O_3 glasses. *Ceramics International*, **40**(9, Part A), 14477-14481.

[10] El-Diasty, F., Abdel Wahab, F. A., & Abdel-Baki, M. (2006). Optical band gap studies on lithium aluminium silicate glasses doped with Cr^{3+} ions. *Journal of Applied Physics*, **100**(9), 093511.

[11] El-Mallawany, R., Dirar Abdalla, M., & Abbas Ahmed, I. (2008). New tellurite glass: Optical properties. *Materials Chemistry and Physics*, **109**(2-3), 291-296.

[12] El-Mallawany, R. (2000). *Tellurite Glasses: Physical Properties and Data*. Florida: CRC Press.

[13] Fatimah, S., Sahar, M. R., Ghoshal, S. K., Ariffin, R. & Hamzah, K. (2014). Optical absorption of erbium doped tellurite glass. *Advanced Materials Research*, **895**, 245-249.

[14] Ghoshal, S. K., Awang, A., Sahar, M. R., & Arifin, R. (2015). Gold nanoparticles assisted surface enhanced Raman scattering and luminescence of Er^{3+} doped zinc-sodium tellurite glass. *Journal of Luminescence*, **159**, 265-273.

[15] Jlassi, I., Elhouichet, H., & Ferid, M. (2011). Thermal and optical properties of tellurite glasses doped erbium. *Journal of Materials Science*, **46**(3), 806-812.

[16] Lin, H., Zhang, Y. Y., & Pun, E. Y. B. (2008). Fluorescence investigation of Ho^{3+} in Yb^{3+} sensitized mixed-alkali bismuth gallate glass. *Spectrochimica Acta A: Molecular and Biomolecular Spectroscopy*, **71**(4), 1547-1550.

[17] Mahraz, Z. A. S., Sahar, M. R. & Ghoshal, S. K. (2014). Influence of Er^{3+} dopants on optical properties of boro-tellurite glass. *Advanced Materials Research*, **895**, 211-215.

[18] Parveen, N., Jali, V. M., & Patil, S. D. (2016). Structure and optical properties of TeO_2-GeO_2 glasses, *Proceedings of 47th IRF International Conference*. 10 January 2016. Pune, India. pp. 70-75.

[19] Rivera, V.A.G., Ledemi, Y., Pereira-da-Silva, M. A., Messaddeq, Y. & Marega Jr, E. (2016). Plasmon-photon conversion to near-infrared emission from Yb^{3+}: (Au/Ag-nanoparticles) in tungsten-tellurite glasses. *Scientific Reports*, **6**, 18464.

[20] Samanta, B., Dutta, D. & Ghosh, S. (2017). Synthesis and different optical properties of Gd_2O_3 doped sodium zinc tellurite glasses. *Physica B: Condensed Matter*, **515**, 82-88.

[21] Saritha, D., Markandeya, Y., Salagram, M., Vithal, M., Singh, A. K. & Bhikshamaiah, G. (2008). Effect of Bi_2O_3 on physical, optical and structural studies of ZnO-Bi_2O_3-B_2O_3 glasses. *Journal of Non-Crystalline Solids*, **354**(52-54), 5573-5579.

[22] Serqueira, E. O., de Morais, R. F. & Dantas, N. O. (2013). Controlling the spectroscopic parameters of Er^{3+}-doped sodium silicate glass by tuning the Er_2O_3 and Na_2O concentrations. *Journal of Alloys and Compounds*, **560**, 200-207.

[23] Sidek, H.A.A., Rosmawati, S., Talib, Z.A., Halimah, M.K. & Daud, W.M. (2009). Synthesis and optical properties of ZnO-TeO_2 glass system. American Journal of Applied Sciences, **6**(8), 1489-1494.

[24] Sidek, H. A. A., El-Mallawany, R., Siti, S. B., Halimah, M. K., & Khamirul, A. M. (2015). Optical properties of erbium zinc tellurite glass system. *Advances in Materials Science and Engineering*, **2015**, Article ID 628954.

[25] Soltani, I., Hraiech, S., Horchani-Naifer, K., Elhouichet, H., Gelloz, B. & Férid, M. (2016). Growth of silver nanoparticles stimulate spectroscopic properties of Er^{3+}-doped phosphate glasses: Heat treatment effect. *Journal of Alloys and Compounds*, **686**, 556-563.

[26] Wang, Y., Dai, S., Chen, F., Xu, T., & Nie, Q. (2009). Physical properties and optical band gap of new tellurite glasses within the TeO_2-Nb_2O_5-Bi_2O_3 system. *Materials Chemistry and Physics*, **113**(1), 407-411.

[27] Yusoff, N. M., Sahar, M. R. & Ghoshal, S. K. (2015). Sm^{3+}: Ag NPs assisted modification in absorption features of magnesium tellurite glass. *Journal of Molecular Structure*, **1079**, 167-172.

[28] Yusof, N. N., Ghoshal, S. K., Ariffin, R. & Sahar, M. R. (2015). Modified absorption features of titania-erbium incorporated plasmonic tellurite glass system. *Jurnal Teknologi*, **76**(13), 89-94.

[29] Żmojda, J., Kochanowicz, M., & Dorosz, D. (2014). Low-phonon tellurite glass co-doped with Tm^{3+}/Ho^{3+} ions for optical fiber technology. *Photonics Letters of Poland*, **6**(2), 56-58.